Adsorption of Sodium Iodine at Air/Water Interface

Cuong V. Nguyen[1], Hiromichi Nakahara[2], Osamu Shibata[3] and Chi M. Phan[4,]*

[1] Faculty of Applied Sciences, Ton Duc Thang University, Hochiminh City, 70000, Vietnam

[2] Department of Industrial Pharmacy, Daiichi University of Pharmacy, 22-1 Tamagawa-cho, Minami-ku Fukuoka 815-8511, Japan

[3]Department of Biophysical Chemistry, Graduate School of Pharmaceutical Sciences, Nagasaki International University, Sasebo, Nagasaki 859-3298, Japan.

[4] Discipline of Chemical Engineering and Curtin Institute of Functional Molecules and Interfaces, Curtin University, GPO Box U1987, Perth, WA 6845, Australia

***Corresponding author:** c.phan@curtin.edu.au

ABSTRACT

The change in surface potential was measured for NaI solutions. The modelled surface charge was then calculated and compared with molecular simulations. It was found that I^- was enhanced at the air/water interface more than Na^+. The result, which was confirmed by simulations, was opposite to the previous observation with NaCl. The trend is also consistent with anionic effects: larger and more polar anions adsorbed stronger at the air/water interface. The theoretical model was applied successfully to describe the changes for both systems, which are positive for NaCl and negative for NaI, respectively. The combined results of the two systems also revealed that the self-ionization of pure water induced a positive surface charge at 16.9 mV.

KEYWORDS: sodium iodine, surface potential, surface charge

Introduction

The adsorption of ions at the air/water interface is crucial to a proper understanding and explanation of various physical and chemical processes, such as mineral flotation [1] and atmospheric aerosols [2]. Thermodynamically, ions are expected to be repelled from the interface as the addition of salt to water triggers an increase in surface tension [3,4]. On the other hand, current studies of the reactivity of a variety of salt solutions have revealed that there exists an enhancement of anions at the liquid/vapour interface [5], which corresponds to the Hofmeister series [6]. Based on measurements of the uptake of gaseous Br_2 and Cl_2 by aqueous interfaces of sodium-halide salt solutions, Hu et al. [7] predicted that Cl^- and Br^- ions must exist at the air/water interface of those solutions. This prediction has been followed by a large number of studies employing molecular dynamics (MD) simulation. Instead of an ion-free interface, MD studies have demonstrated that some specific ions, such as Cl^-, Br^- and I^- exhibit a propensity for the liquid/vapour interface [8–10]. In addition, other studies using state-of-the-art techniques such as second-harmonic generation (SHG), vibrational sum-frequency generation (VSFG) and X-ray photoelectron spectroscopy (XPS) to validate the existence of ions near the surface [11–13]. It is noted that sodium-halide salts impact the structure of hydrogen bonding of water in the interfacial region at the level dependent on the nature of anions.

Combining experimental and computational results, our study has depicted the image of ionic distribution within the interfacial region of NaCl solutions [14]. More importantly, based on the newly proposed diffuse plane, the positively charged interface of NaCl solutions obtained by the measurement of their surface potentials are verified by the interaction between ions and interfacial water molecules acquired from MD simulations. In this study, we quantitatively evaluate the impact of anion nature on surface charge as well as the distribution of ions at the air/water interface by comparing the results of two salt solutions, NaCl and NaI.

Theory

As described in previous study and elsewhere [14,15], the alteration of surface potential of salt solutions can be expressed as a function of surface charge:

$$\Delta V = V - V_0 = \frac{\lambda}{\varepsilon_s \varepsilon_0}\sigma + asinh\left(\frac{\sigma}{\sqrt{8C_b \varepsilon \varepsilon_0 k_B T}}\right)\frac{2k_B T}{e} \quad [1]$$

where

ΔV : change in surface potential (V)

σ : surface charge density (C/m^2)

C_b : bulk particle concentration (particles/m^3)

k_B: Boltzmann constant

T: temperature (K)

e: charge of an electron

ε_s : permittivity of interfacial layer

ε_0 : vacuum permittivity

ε: permittivity of solution

λ : the thickness of the interfacial layer

In the above equation, V_0 is surface potential of pure water. While V_0 is non-zero due to the presence of hydronium/hydroxide ions, its actual value remains unqualified [16]. The solution permittivity, ε, is dependent on the salinity [17]. The dependency is linear for NaCl and NaI up to 1.5 M [18] and is given as:

$$\varepsilon(C_b) = 78.2 - 13.8C_b \quad [2]$$

The change in surface potential can be positive or negative depending on surface charge density of the interface, which is difficult to quantify in case of air/salt solution surface [19]. Previous investigation on the interface of NaCl solution employed MD simulation and directly quantified surface charge via the adsorption of ions:

$$\sigma = eN_a\Gamma_{ion} = eN_a(\Gamma_{cation} - \Gamma_{anion}) \quad [3]$$

where N_a is Avogadro number, Γ_{ion} (mol/m^2) is the net adsorption amount or concentration of ions within the interfacial zone.

Thermodynamically, the adsorption of ions within the interfacial zone is governed by their interaction with surface water molecules, or the asymmetric H-bonds network [20]. The interaction would be influenced by the nature of cations and anions and determine the sign of surface charge density. In case of the NaCl, the number of the adsorbed cations is greater than that of anion, resulting in positive surface charge density [14], which then was verified by experimental surface potential.

Computational and Experimental Methods

Two empty regions representing vacuum (10 nm length each) were placed at both sides of a slab of water layer (with a thickness of 10 nm) to form two air/water interfaces. The simulation employed GROMACS 4.5.5 to generate the molecular trajectories with a time step of 1 fs. Water model SPC/E was used and ions were described by OPLS force field [21,22]. Simulation boxes were formed following a widely accepted procedure. At first, a box 3×3×10 of water molecules was built before replacing a number water molecule by Na^+ and I^- ions for the purpose of increasing NaI concentration from 0 to 1.5 M which is consistent with the experimental values. The box then was simulated at constant temperature (298 K and pressure (1 bar) employing Berendsen barostat with 2 ps relaxation time and 1.3 nm cut-off. Then, the *z*-dimension was extended to 30 nm to created two vacuum regions, while *x*- and *y*-dimension of the box were rescaled correspondingly. Finally, the simulation was run for 30 ns at constant volume and temperature (298 K) employing Nose-Hoover thermostat. Density distribution and water dipole moment were analysed based on the last 10 ns of simulation using GROMACS built-in functions. LINCS algorithms were used to keep the geometry of water molecules. Electrostatic interactions were dealt with by employing Ewald sums.

In order to eliminate the broadening of the interface caused by capillary waves, the method of identifying the truly interfacial molecules (ITIM) [23] was employed for analysing the last 10 ns of production simulation. The ITIM analyses have been conducted using PYTIM package [24]. In this study, neighbouring test lines were separated by 0.4 A from each other based on

the suggestions of previous studies [25–27] in literature. The radius of the probe sphere was defined at 2.0 A, while the atoms' diameter was estimated by their Lennard-Jones distance parameter. The procedure of ITIM analyses was repeated three times, and the molecules and their number densities within the first three outer interfacial layers were determined.

The measurement of surface potential was conducted using an ionizing electrode as described previously [28]. Sodium iodide (purity > 99.5%) was obtained from Nacalai Tesque (Kyoto, Japan) and was used as received. Each measurement was repeated at least 3 times to ensure its repeatability.

Results

This study extended the previous definition of the interfacial zone to NaI solutions. Density distribution of ions and water was obtained by using built-in function analysing the last 10 ns of each simulation. This length of analysing time was proved sufficient and reliable in the previous study [14]. Instead of using Gibbs dividing plane, which is based on water density profile, in this study surface limit is calculated from water dipole moment profile. Specifically, the interfacial zone is defined corresponding to the peak of water dipole order as depicted in **Fig. 1**.

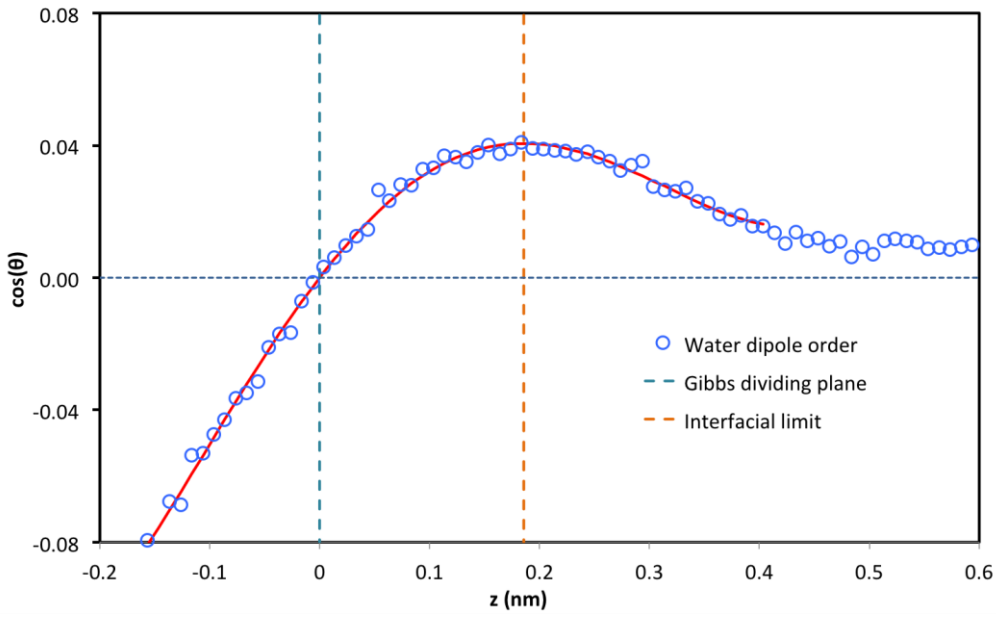

Fig. 1. Water distribution around the interfacial limit.

It should be noted that a newly-defined interfacial limited has been successfully applied to the systems of alcohols aqueous solutions [29], alcohols/NaCl mixture [30] and NaCl solution [14] to quantify the molecular arrangement of the adsorption zone. Most importantly, this limiting plane of interfacial zone helps verify the positive net ionic adsorption at the air/water interface of NaCl solution, which is in contrast to traditional understanding of a negative adsorption at air/liquid interface [15,31], where ions are expected to be depleted from the surface due to the less polarization of outmost interfacial water layer [32]. The interfacial limit is employed to describe the surface adsorption of NaI salt. Similarly, the net ionic adsorption is figured out based on the accumulative number of ions as showed in **Fig. 2**.

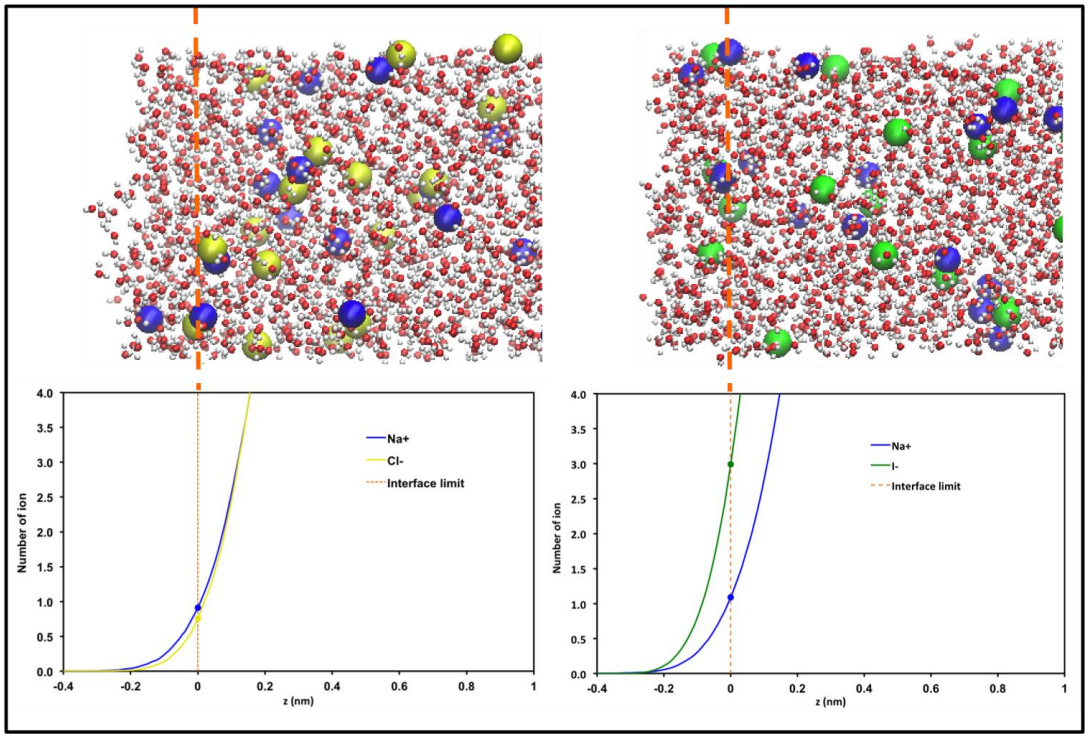

Fig. 2. Accumulative numbers of ions within the interfacial zone. NaCl (left) and NaI (right) at the same concentration (0.74 M)

Ionic adsorption. There is a contradictive behaviour of ions within the interfacial zone between the two systems. In both cases, the numbers of adsorbed Na^+ at the interface are relatively similar. However, the relative anion/cation ratios are different. While the number of adsorbed Cl^- is lower than that of Na^+, there is significantly stronger adsorption of I^- than Na^+ within this

zone. This can be observed clearly on the snapshots of two simulations and result in the negative net charge at the interface of NaI solution.

To exclude the capillary wave from the ionic distribution, number densities of O (water) across the simulation box and the first 3 outmost layers (only the first layer was shown), ions was determined following ITIM method and plotted in **Fig. 3**. Accumulated numbers of ions were also figured out for the purpose of calculating the number of ions within the interfacial zone. It is noted that in this instance, the limit of the interfacial layer was selected as the peak position of the first layer of O (water) by selecting the maximum of the obtained Gaussian distribution of the first layer. This limitation reasonably agreed with the position at which the mass water density is 50% of the bulk density [23]. It can be seen in **Fig. 3** that I^- has higher concentration than Na^+. The data indicated that the relative difference between the ions is not affected by the roughness of water surface.

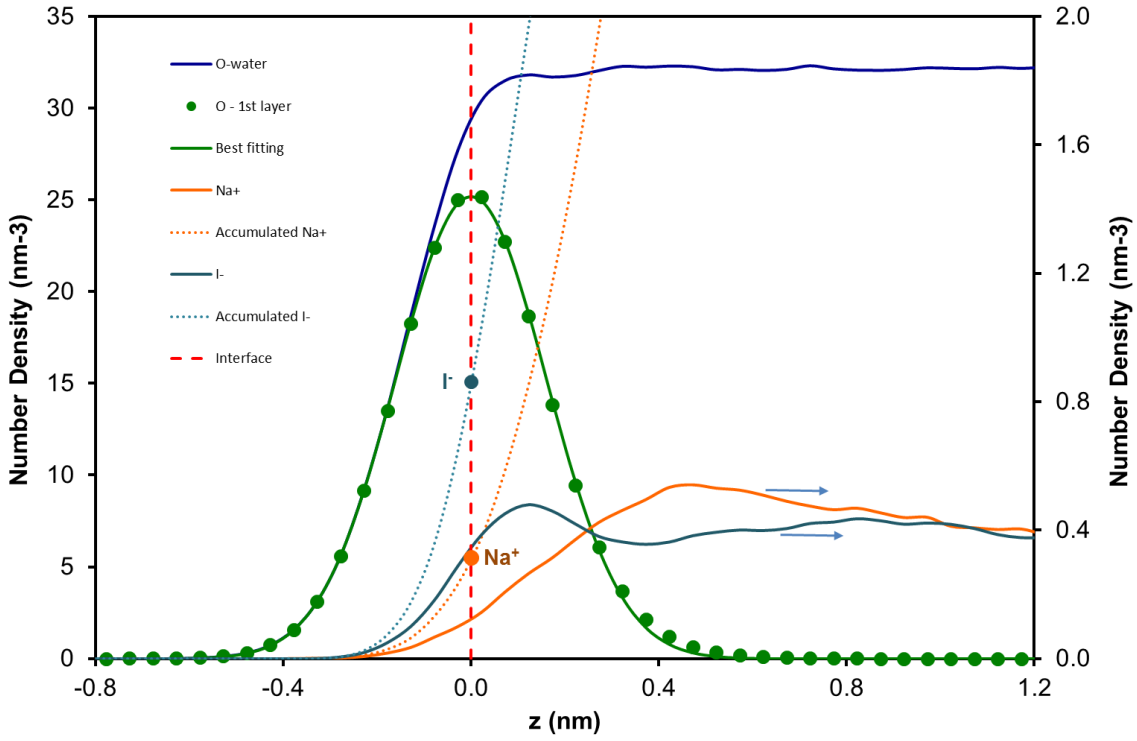

Fig. 3. Number of O (water) in the first layer and throughout the whole simulation box, ions and their accumulation within the interfacial zone (0.74 M NaI).

153

154 The penetration of ions to the interface would be expectedly governed by the interaction with
155 surrounding water molecules. Thus, radial distributions functions (RDF) of water oxygen
156 molecules around ions were analysed and illustrated in **Fig. 4**.

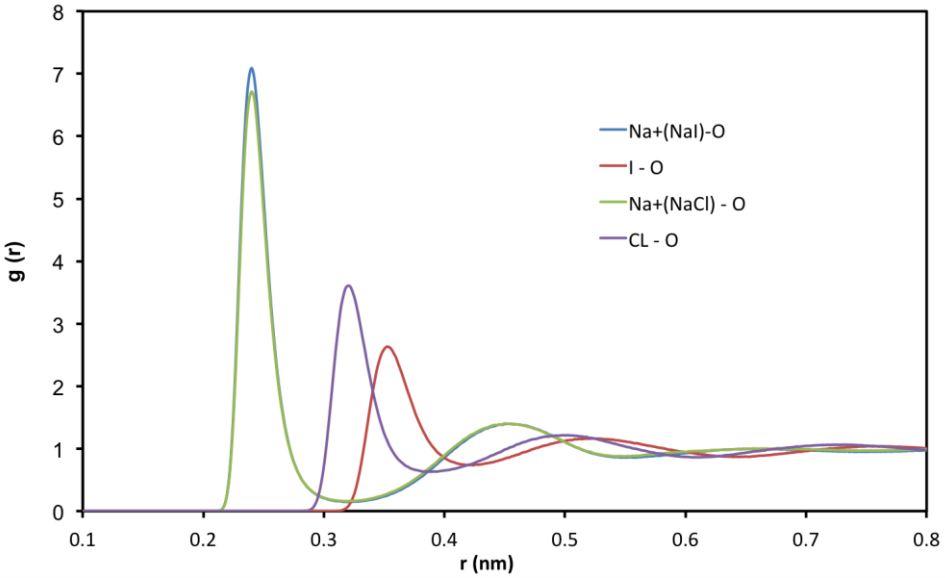

157

158 **Fig. 4**. Radial distribution functions of water oxygen around ions in both NaCl and NaI
159 solutions.

160 **Fig. 4** indicated a stable solvation shell around Na^+ ions in both solutions, which would be
161 responsible for almost similar adsorption of this cation at the interface regardless of different
162 companion anions. Nevertheless, the hydration layer of I^- was less concentrated at a further
163 distance than that of Cl^-. This would be driven by a larger ionic radii [33] of I^-. Recently, it has
164 been shown the hydration shell of ions has a negative contribution to the surface tension by
165 interaction to surface water layer [34]. The observed trend follows the "hardness" order within
166 the Hofmeister series [3] and variation in Na^+ penetration depth with different anions [35].

167
168
169

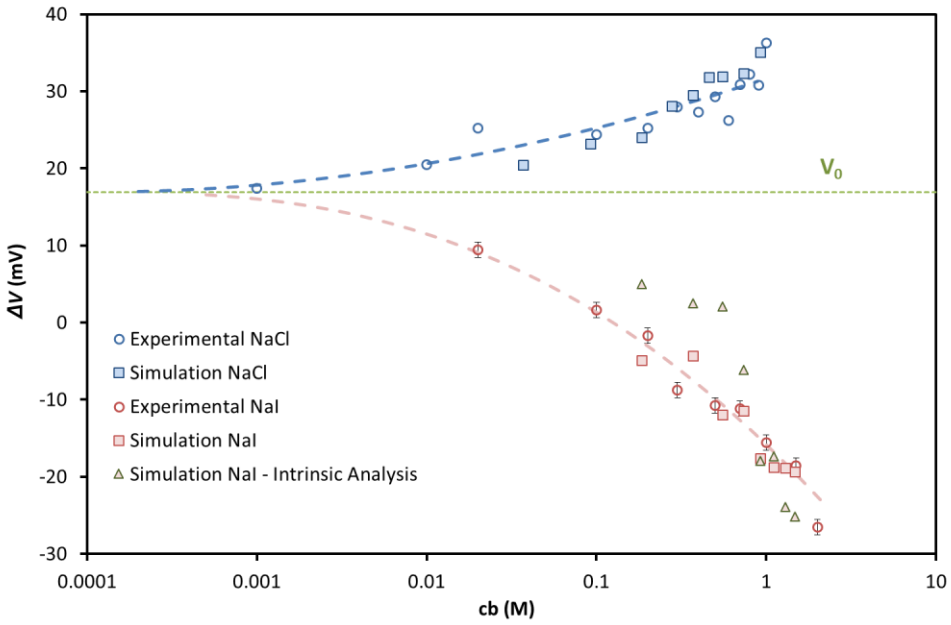

Fig. 5. Change in surface potential for NaI and NaCl solutions with an asymptotic limit at $C_b \rightarrow 0$. The data for NaCl was taken from the previous study [14]. Lines are asymptotic curves. The best-fitted of $\lambda/\varepsilon\varepsilon_s$ for NaI simulation was determined at 0.3 and 1.8 F/m^2, for *z*-axis distribution and ITIM analysis respectively.

Surface charge. The contrasting behaviour between I^- and Cl^- is also evident by the change in surface potential data (**Fig. 5**). In Eq.(1), the value of ΔV represents the re-organization of water dipole moment by salts. Hence, ΔV should approach zero as $C_b \rightarrow 0$. However, it can be seen in **Fig.4b** that ΔV does not approach zero as C_b approach zero. By empirical fitting to both NaCl and NaI data, the asymptotic value was determined at 16.9 mV.

To corroborate the simulation with experimental data, the surface charge in **Fig.4** was calculated by Eq. (1) and Eq. (2). The change in surface potential was adjusted by 16.9 mV to account for the pure water surface. The surface charge was also obtained via simulation (Fig. 5). Both methods, density distribution and intrinsic analyses, demonstrated a negative surface charge, i.e. enhancement of I^- over Na^+. The charge is increased with increasing NaI concentration. The experimental and simulation data verified the contrasting behaviour between NaCl and NaI. It is noteworthy that previous simulations showed similar effects of anions: I^- is far more enhanced than Cl^- near the surface [10]. However, the previous simulation showed that Cl^- was also more enhanced than Na^+, which is contrasting to our results [14].

Hence the simulated surface charge of NaCl solution is model-dependent. It should be emphasized that the enhancement of Na^+ over Cl^- was consistent with the experimental data, which showed a positive charge. In both simulations, the relative difference NaCl is much small than that of NaI, as demonstrated with Fig.6 and Fig.1 of Jungwirth and Tobias simulation [10]. In summary, the simulated ratio of Na^+/Cl^- is small and model-dependent. The simulated ratio of Na^+/I^- is much larger, with a significant enhancement of I^-, and consistent with the experimental data.

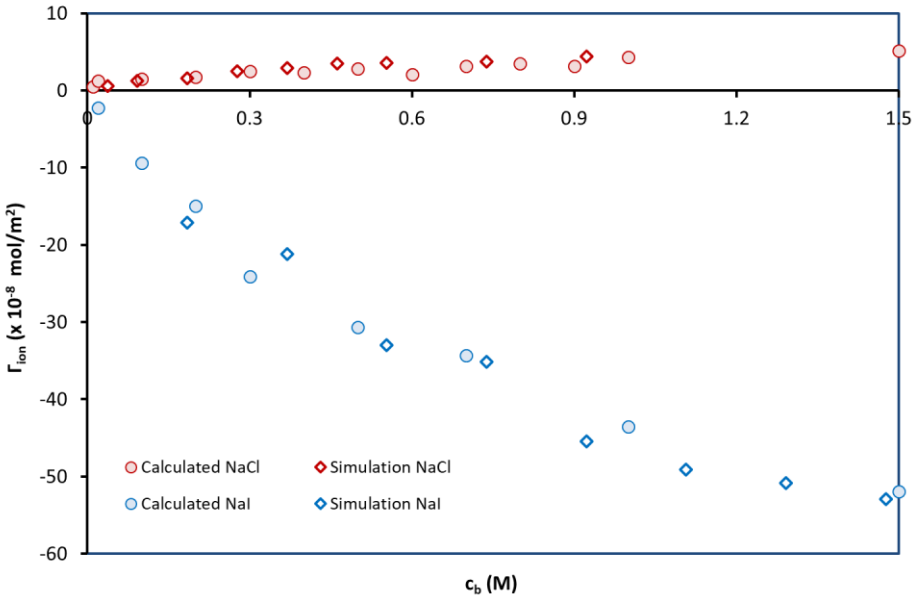

Fig. 6. Net ionic adsorption within the interfacial layer of NaI and NaCl solutions.

It can be seen from **Fig. 6** that experimental and simulation data are consistent for both NaI and NaCl. For the fitting, equation (3) has one parameter, $\lambda/\varepsilon\varepsilon_s$, which incorporate the thickness and pemissivity of the interfacial layer. Since these properties cannot be quantified from simulation, the value are obtained by fitting against the experimental data.

The value of $\lambda/\varepsilon\varepsilon_s$ for NaI (**Fig. 5**) was determined at 0.3 F/m^2, which is much smaller than that of NaCl [14]. This can be explained by the "harder" hydration shell of I^-. As mentioned above, I^- hydration shell has low polarization [9] and larger radii [33], which can increase λ and

decrease ε_s. The interaction of this hydration shell with surface water [34] can significantly reduce the permittivity of the surface layer, ε_s, as well.

Finally, it should be noted that the asymptotic value of surface potential is positive, which can be attributed to the water orientation [36] or the relatively enhancement between hydronium/ hydroxide ions at the pure water surface [37]. However, the *absolute* value for ionic adsorption for pure water is only obtainable from Eq.(1) if the value of $\lambda/\varepsilon\varepsilon_s$ is known.

Conclusions

In summary, we investigated experimentally and theoretically the adsorption of NaI at the air/water interface. It was consistently confirmed by both methods that I^- has a higher adsorption than Na^+. The relative arrangement was opposite to the NaCl system, which can be attributed to a larger hydration shell of I^-. The results quantify the ionic effect, in this case halide ions, on surface adsorption and surface potential. The results also validate the role of the water surface structure in defining the limit of the interfacial layer. More interestingly, the study with these electrolytes also indicates that the surface potential of pure water is positive, at 16.9 mV.

AUTHOR INFORMATION

The authors declare no competing financial interests.

REFERENCES

[1] C.V. Nguyen, C.M. Phan, H.M. Ang, H. Nakahara, O. Shibata, Y. Moroi, Surface potential of 1-hexanol solution: Comparison with methyl isobutyl carbinol, J. Phys. Chem. B. 117 (2013). doi:10.1021/jp4027157.

[2] V. Ramanathan, P.J. Crutzen, J.T. Kiehl, D. Rosenfeld, Aerosols, Climate, and the Hydrological Cycle, Sci. 294 (2001) 2119.

[3] L.M. Pegram, M.T. Record, Hofmeister Salt Effects on Surface Tension Arise from Partitioning of Anions and Cations between Bulk Water and the Air−Water Interface, J. Phys. Chem. B. 111 (2007) 5411–5417. doi:10.1021/jp070245z.

[4] P.B. Petersen, On the nature of ions at the liquid water surface, Annu. Rev. Phys. Chem. 57 (2006) 333.

[5] L. Sun, X. Li, Y. Tu, H. Agren, Origin of ion selectivity at the air/water interface, Phys. Chem. Chem. Phys. 17 (2015) 4311–4318. doi:10.1039/C4CP03338H.

[6] P. Jungwirth, P.S. Cremer, Beyond Hofmeister, Nat. Chem. 6 (2014) 261. doi:10.1038/nchem.1899.

[7] J.H. Hu, Q. Shi, P. Davidovits, D.R. Worsnop, M.S. Zahniser, C.E. Kolb, Reactive Uptake of Cl2(g) and Br2(g) by Aqueous Surfaces as a Function of Br- and I- Ion

Concentration: The Effect of Chemical Reaction at the Interface, J. Phys. Chem. 99 (1995) 8768–8776. doi:10.1021/j100021a050.

[8] P. Jungwirth, D.J. Tobias, Specific ion effects at the air/water interface, Chem. Rev. 106 (2006) 1259–1281.

[9] P. Jungwirth, D.J. Tobias, Ions at the Air/Water Interface, J. Phys. Chem. B. 106 (2002) 6361–6373. doi:10.1021/jp020242g.

[10] P. Jungwirth, D.J. Tobias, Molecular Structure of Salt Solutions: A New View of the Interface with Implications for Heterogeneous Atmospheric Chemistry, J. Phys. Chem. B. 105 (2001) 10468–10472. doi:10.1021/jp012750g.

[11] E.A. Raymond, G.L. Richmond, Probing the Molecular Structure and Bonding of the Surface of Aqueous Salt Solutions, J. Phys. Chem. B. 108 (2004) 5051–5059. doi:10.1021/jp037725k.

[12] D. Liu, G. Ma, L.M. Levering, H.C. Allen, Vibrational Spectroscopy of Aqueous Sodium Halide Solutions and Air−Liquid Interfaces: Observation of Increased Interfacial Depth, J. Phys. Chem. B. 108 (2004) 2252–2260. doi:10.1021/jp036169r.

[13] S. Ghosal, J.C. Hemminger, H. Bluhm, M. Bongjin Simon, et al., Electron Spectroscopy of Aqueous Solution Interfaces Reveals Surface Enhancement of Halides, Science (80-.). 307 (2005) 563–566.

[14] C. V. Nguyen, C.M. Phan, H. Nakahara, O. Shibata, Surface structure of sodium chloride solution, J. Mol. Liq. 248 (2017) 1039–1043. doi:10.1016/j.molliq.2017.10.138.

[15] H.-J. Butt, K. Graf, M. Kappl, Physics and chemistry of interfaces, John Wiley & Sons, 2006.

[16] R. Zimmermann, U. Freudenberg, R. Schweiß, D. Küttner, C. Werner, Hydroxide and hydronium ion adsorption - A survey, Curr. Opin. Colloid Interface Sci. 15 (2010) 196–202. doi:10.1016/j.cocis.2010.01.002.

[17] C.T. Swift, An Improved Model for the Dielectric Constant of Sea Water at Microwave Frequencies, IEEE J. Ocean. Eng. 2 (1977) 104–111. doi:10.1109/JOE.1977.1145319.

[18] A. Levy, D. Andelman, H. Orland, Dielectric constant of ionic solutions: A field-theory approach, Phys. Rev. Lett. 108 (2012). doi:10.1103/PhysRevLett.108.227801.

[19] S.M. Kathmann, I.F.W. Kuo, C.J. Mundy, G.K. Schenter, Understanding the Surface Potential of Water, J. Phys. Chem. B. 115 (2011) 4369–4377. doi:10.1021/jp1116036.

[20] F. Perakis, L. De Marco, A. Shalit, F. Tang, Z.R. Kann, T.D. Kühne, R. Torre, M. Bonn, Y. Nagata, Vibrational Spectroscopy and Dynamics of Water, Chem. Rev. 116 (2016) 7590–7607. doi:10.1021/acs.chemrev.5b00640.

[21] W.L. Jorgensen, D.S. Maxwell, J. Tirado-Rives, Development and testing of the OPLS all-atom force field on conformational energetics and properties of organic liquids, J. Am. Chem. Soc. 118 (1996) 11225–11236.

[22] G.A. Kaminski, R.A. Friesner, J. Tirado-Rives, W.L. Jorgensen, Evaluation and Reparametrization of the OPLS-AA Force Field for Proteins via Comparison with Accurate Quantum Chemical Calculations on Peptides, J. Phys. Chem. B. 105 (2001) 6474–6487. doi:10.1021/jp003919d.

[23] L.B. Pártay, G. Hantal, P. Jedlovszky, Á. Vincze, G. Horvai, A new method for determining the interfacial molecules and characterizing the surface roughness in computer simulations. Application to the liquid-vapor interface of water, J. Comput. Chem. 29 (2008) 945–956. doi:10.1002/jcc.20852.

[24] M. Sega, G. Hantal, B. Fábián, P. Jedlovszky, Pytim: A python package for the interfacial analysis of molecular simulations, J. Comput. Chem. (2018). doi:10.1002/jcc.25384.

[25] M. Sega, The role of a small-scale cutoff in determining molecular layers at fluid interfaces, Phys. Chem. Chem. Phys. 18 (2016) 23354–23357. doi:10.1039/c6cp04788b.

[26] M. Jorge, G. Hantal, P. Jedlovszky, M.N.D.S. Cordeiro, A critical assessment of methods for the intrinsic analysis of liquid interfaces: 2. Density profiles, J. Phys. Chem. C. 114 (2010) 18656–18663. doi:10.1021/jp107378s.

[27] R.A. Horváth, B. Fábián, M. Szőri, P. Jedlovszky, Investigation of the liquid-vapour interface of aqueous methylamine solutions by computer simulation methods, J. Mol. Liq. 288 (2019) 110978. doi:10.1016/J.MOLLIQ.2019.110978.

[28] C. V Nguyen, C.M. Phan, H.M. Ang, H. Nakahara, O. Shibata, Y. Moroi, Molecular Dynamics Investigation on Adsorption Layer of Alcohols at the Air/Brine Interface, Langmuir. 31 (2015) 50–56. doi:10.1021/la504471q.

[29] C.M. Phan, C. V Nguyen, T.T.T. Pham, Molecular Arrangement and Surface Tension of Alcohol Solutions, J. Phys. Chem. B. (2016). doi:10.1021/acs.jpcb.6b01209.

[30] G. Gao, C. V. Nguyen, C.M. Phan, Molecular arrangement between electrolyte and alcohol at the air/water interface, J. Mol. Liq. 242 (2017) 859–867. doi:10.1016/j.molliq.2017.07.083.

[31] O. Björneholm, M.H. Hansen, A. Hodgson, L.-M. Liu, D.T. Limmer, A. Michaelides, P. Pedevilla, J. Rossmeisl, H. Shen, G. Tocci, E. Tyrode, M.-M. Walz, J. Werner, H. Bluhm, Water at Interfaces, Chem. Rev. 116 (2016) 7698–7726. doi:10.1021/acs.chemrev.6b00045.

[32] L. Onsager, N.N.T. Samaras, The Surface Tension of Debye-Hückel Electrolytes, J. Chem. Phys. 2 (1934) 528–536. doi:10.1063/1.1749522.

[33] Y.Z. Wei, P. Chiang, S. Sridhar, Ion size effects on the dynamic and static dielectric properties of aqueous alkali solutions, J. Chem. Phys. 96 (1992) 4569–4573. doi:10.1063/1.462792.

[34] G. Hantal, M. Sega, G. Horvai, P. Jedlovszky, Contribution of Different Molecules and Moieties to the Surface Tension in Aqueous Surfactant Solutions, J. Phys. Chem. C. (2019) acs.jpcc.9b02553. doi:10.1021/acs.jpcc.9b02553.

[35] H. Tissot, G. Olivieri, J.J. Gallet, F. Bournel, M.G. Silly, F. Sirotti, F. Rochet, Cation Depth-Distribution at Alkali Halide Aqueous Solution Surfaces, J. Phys. Chem. C. 119 (2015) 9253–9259. doi:10.1021/jp512695c.

[36] Y.R. Shen, V. Ostroverkhov, Sum-frequency vibrational spectroscopy on water interfaces: Polar orientation of water molecules at interfaces, Chem. Rev. 106 (2006) 1140–1154. doi:10.1021/cr040377d.

[37] V. Buch, A. Milet, R. Vacha, P. Jungwirth, J.P. Devlin, Water surface is acidic, Proc. Natl. Acad. Sci. 104 (2007) 7342–7347. doi:10.1073/pnas.0611285104.